

Preparation of zinc oxide films by an electrostatic spray deposition process

Ju-Hyun Jeong^{a,b}, Young-Sun Jeon^{a,b}, Kyung-Ok Jeon^{a,b}, Kyu-Seog Hwang^a and Byung-Hoon Kim^{b,*}

^aDepartment of Applied Optics and Institute of Photoelectronic Technology, 864-1 Wolgye-dong, Gwangsan-gu, Gwangju 506-824, Korea

^bDepartment of Materials Science & Engineering, Chonnam National University, 300 Yongbong-dong, Buk-gu, Gwangju 500-757, Korea

Highly transparent ZnO thin films were made by electrostatic spray deposition for 60 minutes-120 minutes at 400 °C on soda-lime-silica slide glass substrates. The peaks in the X-ray diffraction analysis could be indexed as from the structure of crystalline zinc oxide. From surface observations using a field emission scanning electron microscope and scanning probe microscope, the surface morphology of the films was found to depend chiefly on depositing time. All the films exhibit a high transmittance (> 80%) in the visible region, except for the film deposited for 120 minutes. The band gap values of the ZnO films deposited for various time are found to be 3.25-3.27 eV.

Key words: ZnO thin film, Electrostatic spray deposition, Surface morphology, Transmittance.

Introduction

Zinc oxide (ZnO) is an n-type semiconductor with a wide band gap of 3.3 eV, showing attractive electrical and optical properties. As a wide band gap material, ZnO has received an increasing amount of attention due to its possible applications in ultraviolet (UV) light-emitting devices, electron-acoustic devices, UV detectors, etc. [1-4]. In recent years, there has been considerable interest in the development of high-quality ZnO films to obtain strong UV emission. Several techniques are being used to produce ZnO films; e.g., chemical vapor deposition, molecular beam epitaxy, radio frequency magnetron sputtering, and a sol-gel process [5-8].

Electrostatic spray deposition (ESD) [9-10] is capable of dividing a liquid into fairly uniform and well-distributed droplets with dimensions that can be controlled from several micrometers down to the nanometer range. It has been successfully introduced by Chen et al. as a new film fabrication techniques for ceramic film deposition [11]. Compared with other film fabrication techniques, ESD offers attractive advantages of easy control of film composition, easy control of substrate temperature during deposition, high film growth rate, simple setup, low cost, compatibility with micro-fabrication technology and suitability for thick film preparation.

An ESD process makes use of the electrohydro-

dynamic generation and breaking-up of a Taylor cone of a precursor solution at the outlet of a nozzle to form a very fine spray. The spray is then directed at a heated substrate, leading to film deposition. This is different from conventional spray processes, in that the spray in an ESD process consists of mainly charged droplets, which may be monosized when generated [11]. It is a promising route for the synthesis of dense as well as porous thin films at relatively low deposition temperatures and, thereby, lower materials processing and fabrication costs.

Here, we present the results of ZnO thin films prepared by ESD. We investigated crystallinity, surface morphology, transmittance in the visible spectra range, and energy band gaps of the films in relation to coating time.

Experimental Procedure

A homogeneous precursor solution was prepared by mixing zinc acetate [(CH₃COO)₂Zn·2H₂O] and 2-methoxyethanol (HOCH₂OCH₃). Since zinc acetate has a low solubility in 2-methoxyethanol, 2-aminoethanol (H₂HCH₂CH₂OH) (MEA) was added to obtain a clear solution (concentration: 0.6 mol zinc acetate/1000 ml 2-methoxyethanol). The molar ratio of MEA to zinc acetate was fixed at 1.0. The mixing solution was stirred for 2 h to obtain a homogeneous solution.

Deposition of ZnO films was performed using an ESD setup with a vertical configuration. The details of the setup used have been reported before [12]. A stainless steel needle (0.1 mm and 0.23 mm inner and outer diameter, respectively) was connected to a syringe pump (KD200, KD Scientific Inc., U.S.A.) using a

*Corresponding author:
Tel : +82-62-530-1711
Fax: +82-62-530-1699
E-mail: bhkim@chonnam.ac.kr

silicon rubber tube. The flow rate of the precursor sol was kept at 0.2 ml/60 minutes. In order to obtain a stable cone-jet mode of electrostatic atomization, a high voltage (20 kV) was applied between the needle tip and ground electrode using a DC power supply (SHV120-30K-RD, Converttech Co. Ltd., South Korea). Soda-lime-silica glass (SLSG) cleaned in a H_2O_2 solution, and rinsed in methanol were used as substrates. SLSG substrates on the ground electrode were heated at 400 °C for 60 minutes, 80 minutes, 100 minutes and 120 minutes during spraying. A precursor solution was pumped through the nozzle which was placed 10 cm above the substrates.

The crystal structure of the coated films was characterized by high-resolution X-ray diffraction (HRXRD, X'pert PRO, Philips, Netherlands). The morphology of the films was examined by means of a field emission scanning electron microscope (FE-SEM, S-4700, Hitachi Co., Japan). A scanning probe microscope (SPM, XE-200, PSIA, Korea) was adopted to analyze the surface roughness of the films. Transmittance in the visible spectra region was analyzed by ultra violet (UV) spectrophotometer (Cary 500 Scan, Varian Co., Australia). The thickness of the annealed film was approximately 0.6-0.7 μm , as determined by observation of fracture cross-sections using a FE-SEM.

Results and Discussion

Figure 1 shows XRD spectra of ZnO films on SLSG substrates at 400 °C for 60 minutes-120 minutes. Films deposited at other times reveal the same pattern, except for the intensity between peaks from ZnO, which vary depending on the crystallinity. Broad diffraction peaks

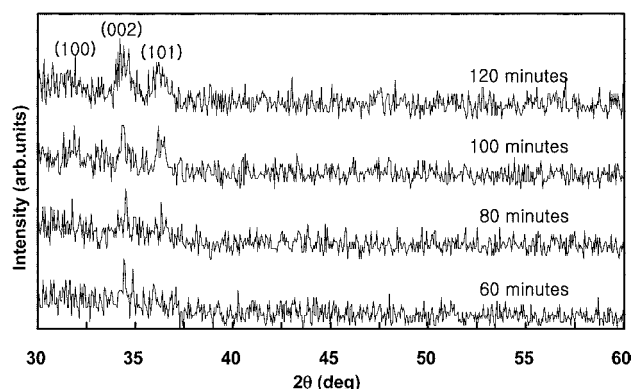


Fig. 1. XRD spectra of the ZnO films on SLSG substrates at 400 °C for various deposition times.

from (100), (002) and (101), corresponding to zinc oxide, were observed; accordingly, the diffraction peaks can be indexed in terms of the structure of crystalline zinc oxide. This result indicates that the ZnO prepared by ESD at 400 °C for above 60 minutes was in a relatively crystalline phase.

Figure 2 shows the FE-SEM images of the ZnO thin films. The ZnO thin films prepared at 400 °C by the ESD process contained some particles. With an increase of deposition time from 60 minutes to 120 minutes, an increasing number of particles was found on the film surface. The particle size increases with increasing deposition time. From a previous report by Chen and co-workers [11], the formation of the dense layer morphology was a clear indication that the solvent in the spray droplets has not been evaporated completely when arriving at the substrate surface. The droplet solution might have spread on the substrate surface and formed a continuous layer.

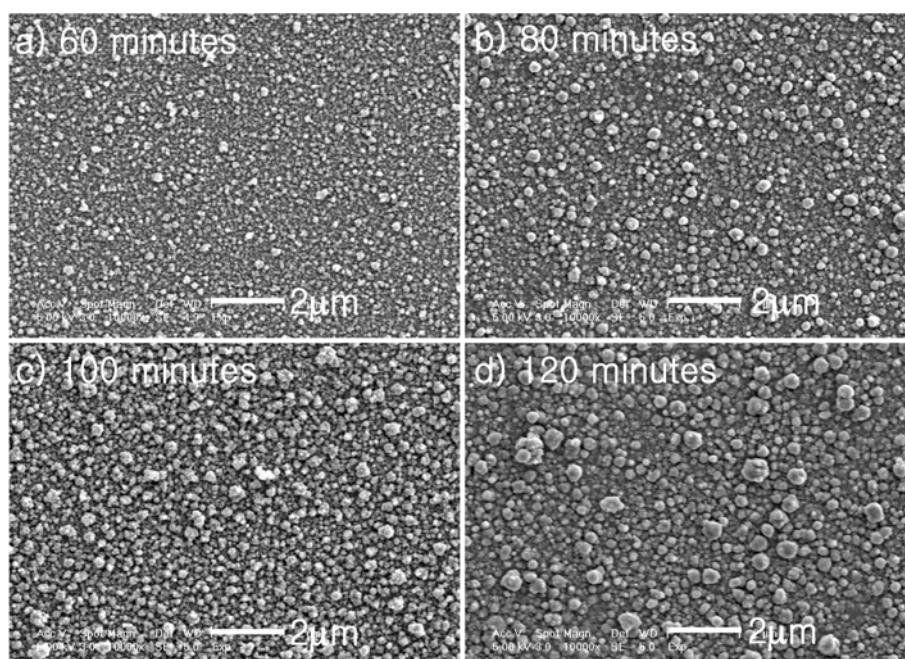


Fig. 2. FE-SEM images of the ZnO films on SLSG substrates at 400 °C for various deposition times.

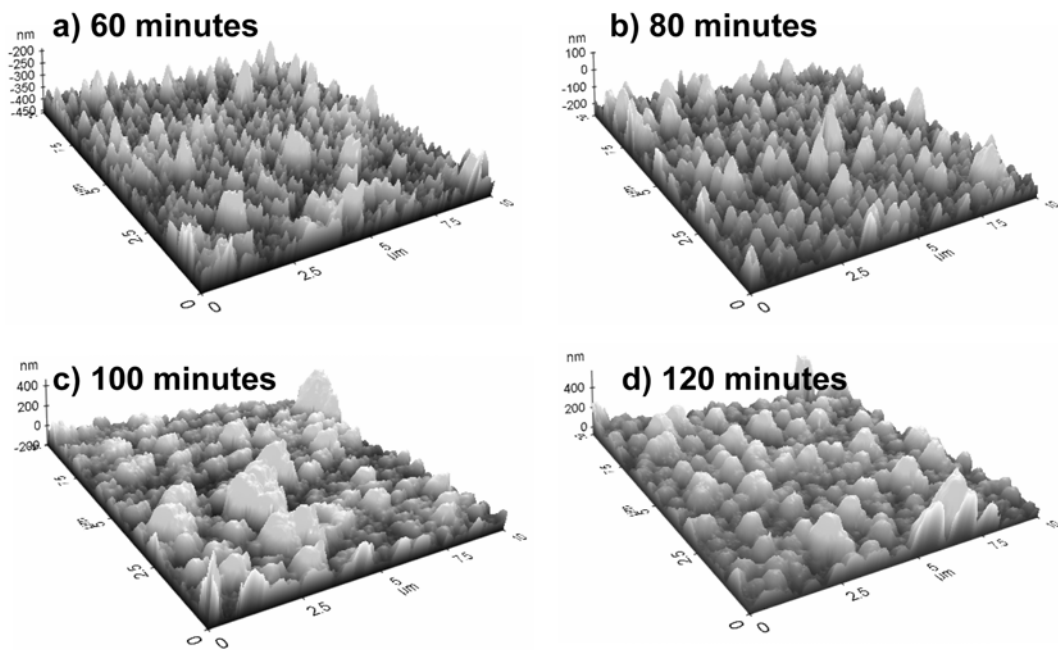


Fig. 3. SPM images of the ZnO films on SLSG substrates at 400°C for various deposition times.

At deposition temperatures where the incoming droplets are still wet but give sufficiently high evaporation and decomposition rates which remain during deposition, the spreading of the droplets on the substrate

surface will lead to a continuous layer. With increasing deposition time, the spreading of the solution droplets will occur on the surface of the layer formed which has a surface tension different from that of the substrate.

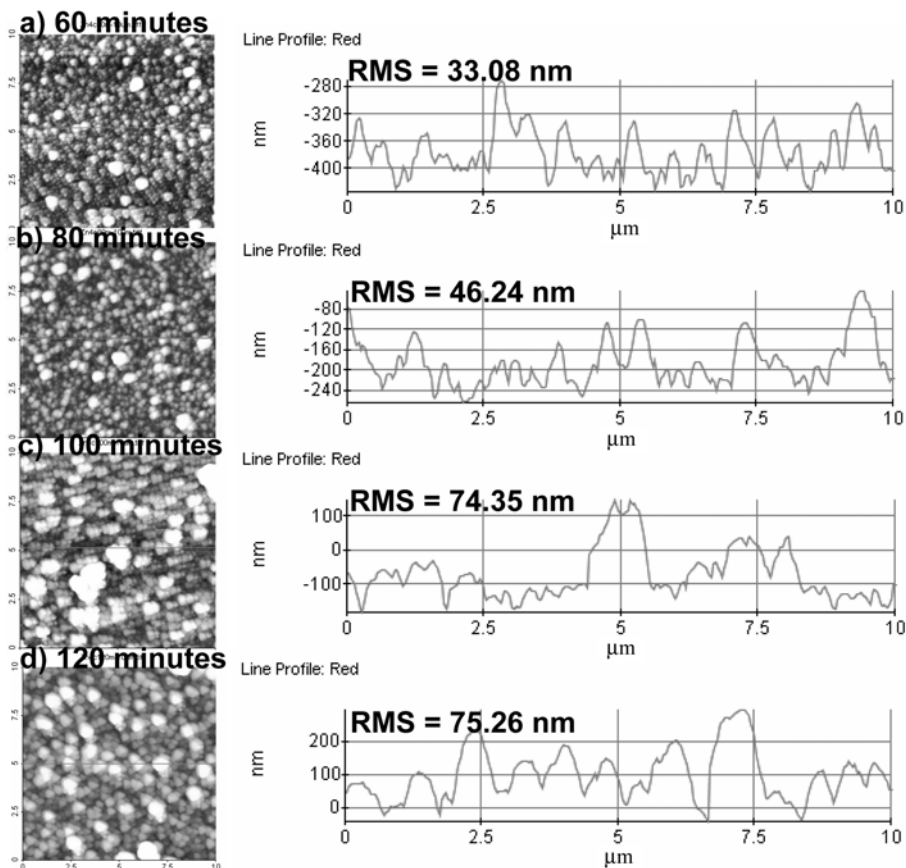


Fig. 4. SPM top-view images and roughness profiles of the ZnO films on SLSG substrates at 400°C for various deposition times.

The wettability of the solution on the deposited layer is less than that on the substrate. Therefore, with an increase of the coating time at the same working temperature, a slower spreading of the droplets will occur and discrete particles may be formed which may increase the surface roughness [13].

Figure 3 shows the SPM images ($10 \times 10 \mu\text{m}^2$) of ZnO films deposited for 60 minutes (a), 80 minutes (b), 100 minutes (c), and 120 minutes (d) at 400°C . Films deposited for 60 minutes and 80 minutes showed needle-shaped grains. While increasing the deposition time up to 100 minutes and 120 minutes, large grain growth was easy to identify, although the grain size uniformly increased. It was observed that with an increase in deposition time to above 100 minutes, the grains gradually converted to round-shaped peaks.

Figure 4 shows SPM top-view images and surface roughness profiles of ZnO films as a function of deposition time. By increasing the deposition time, i.e., above 100 minutes, the root mean square (RMS) roughness was increased to 74.35 nm and 75.26 nm. From previous FE-SEM and SPM results as shown in Figs. 2 and 3, and by increasing the deposition time from 60 minutes and 80 minutes to above 100 minutes, the particle size on the film surface increases and substantial grain growth was easily observed. We assume that grain growth and large particles may be formed by an increase of deposition time, resulting in higher RMS roughness as shown in Fig. 4. The largest rough surface RMS roughness=75.26 nm of the films formed at 400°C for 120 minutes was observed. The surface morphology of the films was found to depend chiefly on deposition time. Optimum surface morphology, i.e., a smooth and homogeneous texture, was obtained with short deposition time.

Figure 5 shows transmission spectra of the ZnO films deposited for different times. All the films exhibited a high transmittance ($> 80\%$) in the visible region, except for the film deposited for 120 minutes, and showed a sharp fundamental absorption edge at about $0.38\text{-}0.40 \mu\text{m}$, which is very close to the intrinsic band-gap of bulk ZnO. The transmittance is expected to depend mainly on three factors, [14] i.e., (1) oxygen deficiency; because films deposited by electron-beam evaporation are brownish in color with poor transparencies [14], (2) surface roughness; surface scattering reduces the transmittance which depends on the grain size, and (3) impurity centers. We can assume that the lower transmittance of the film with an increase of deposition time is mainly due to the surface roughness of the film, as shown in Fig. 4.

Furthermore, we calculated the bandgap values of the films from their transmission spectra using the following equation [15]:

$$\alpha = (h\nu - E_g)^{1/2}$$

where α is the absorption coefficient, E_g is the band

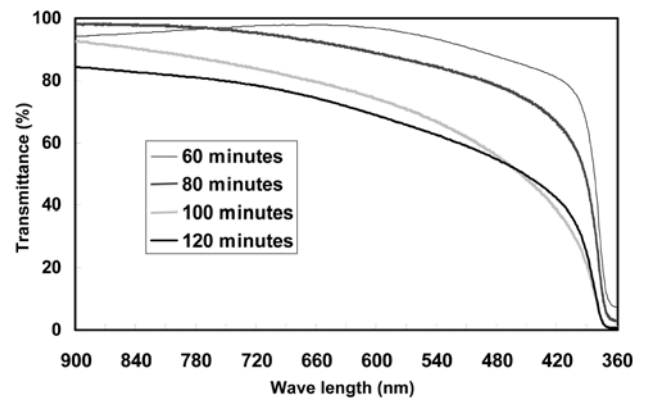


Fig. 5. Transmittance of the ZnO films on SLSG substrates at 400°C for various deposition times.

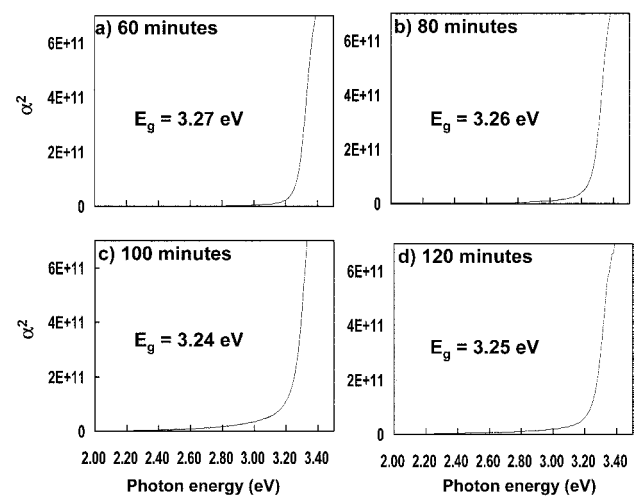


Fig. 6. Square of the absorption coefficient as a function of the photon energy for the ZnO films on SLSG substrates at 400°C for various deposition times.

gap and $h\nu$ is the photon energy. The intersection of the linear region on the $h\nu$ axis of the plot of α^2 versus $h\nu$ gives the band gap of the ZnO films deposited on SLSG substrates. As shown in Fig. 6, using this method [15] the bandgap values of the ZnO films deposited for various times are found to be 3.25-3.27 eV. The change in the optical bandgap is comparatively small but a minimum is shown for the film deposited for 120 minutes.

Conclusions

ZnO thin films having a high transmittance in the visible spectra region were deposited on SLSG substrates by an ESD process. The ZnO prepared by ESD at 400°C for above 60 minutes was in a relatively crystalline state. With an increase of deposition time from 60 minutes to 120 minutes, an increasing number of particles were found on the film surface. The optimum surface morphology, i.e., a smooth and homogeneous texture, was obtained with a short deposition time. All

the films exhibit a high transmittance (> 80%) in the visible region, except for the film deposited for 120 minutes, and show a sharp fundamental absorption edge at about 0.38-0.40 μm .

References

1. Y. Chen, H. Ko, S. Hong, and T. Yao, *Appl. Phys. Lett.* 76[5] (2000) 559-561.
2. Y. Chen, H. Ko, S. Hong, T. Yao, and Y. Segawa, *J. Cryst. Growth* 214/215 (2000) 87-91.
3. A.B.M. Ashrafi, B. Zhang, N. Ninh, K. Wakatsuki, and Y. Segawa, *Jpn. J. Appl. Phys.* 43 (2004) 1114-1117.
4. M. Chen, Z. Pei, X. Wang, C. Sun, and L. Wen, *J. Mater. Res.* 16[7] (2001) 2118-2123.
5. B. Zhao, H. Yang, G. Du, X. Fang, D. Liu, C. Gao, X. Liu, and B. Xie, *Semicond. Sci. Tech.* 19 (2004) 770-773.
6. Y. Chen, S. Hong, H. Ko, M. Nakajima, and T. Yao, *Appl. Phys. Lett.* 76[2] (2000) 245-247.
7. C. Lin, C. Hsiao, S. Chen, and S. Cheng, *J. Electrochem. Soc.* 151[5] (2004) G285-G288.
8. D. Mondelaers, G. Vanhoyland, H. Rul, J. D'haen, M. Bael, J. Mullens, and L. Pouche, *J. Sol-Gel Sci. & Tech.* 26 (2003) 523-526.
9. K. Choy, *Mater. Sci. and Eng. C16* (2001) 139-145.
10. R. Chandrasekhar, and K. Choy, *Thin Solid Films* 398-399 (2001) 59-64.
11. C. Chen, K. Varhaug, and J. Schoonman, *J. Mater. Syn. and Proc.* 4[3] (1996) 189-194.
12. B. Kim, J. Jeong, Y. Jeon, K. Jeon, and K. Hwang, submitted to *J. Sol-Gel Sci. & Tech.* (2005).
13. N. Stelzer, and J. Schoonman, *J. Mater. Syn. and Proc.* 4[6] (1996) 429-438.
14. V. Gupta and A. Mansingh, *J. Appl. Phys.* 80[2] (1996) 1063-1073.
15. K. Hwang, Y. Jeon, B. Kang, K. Nishio, T. Tsuchiya, J. An, and B. Kim, *J. Kor. Phys. Soc.* 46[2] (2005) 521-526.